Characteristics and Annealing Behavior of Polyethylenes Designed for Use as Underground Insulation

Y. D. LEE and P. J. PHILLIPS, *Department of Materials Science and Engineering, University of Tennessee, Knoxville, Tennessee 37996-2200*

Synopsis

A series of polyethylenes developed for use as high voltage electric cable insulation have been studied. All crosslinked polyethylene materials show similar thermal aging characteristics, whereas linear low-density polyethylene is susceptible to thermal aging at higher annealing temperatures. Tree-retardant additives are soluble in xylene, but some are also attached to the gel network. They function both as enhanced antioxidants and as enhancers of electric breakdown strength. Biaxially oriented film shows the greatest resistance to electric breakdown.

INTRODUCTION

There have been many attempts to reduce or eliminate treeing in polymeric insulation ever since the treeing problem was noted in cable insulation. These approaches can be divided into two groups. One is the modification of the cable construction method, and the other is the modification of material or material structure, often with the aid of additives. A major achievement in the latter category was the introduction of crosslinked polyethylene as an insulation material. This offered higher temperature service and improved chemical resistance over the uncrosslinked counterparts.[1] At first, the improvement of electrical properties and resistance to treeing phenomena were attributed to crosslinking. However, several workers suggested that the improvement resulted from the presence of acetophenone, one of several chemical byproducts from the peroxide crosslinking reaction.[2] Other additives have been used for the purpose of reducing treeing by capturing energetic electrons chemically, retarding propagation of trees electrically, and interfering physically with tree propagation. Detailed mechanisms with various additives were reviewed by Eichhorn.[3] Commercially, several grades of polyethylene have been introduced. Among these materials are tree-retardant crosslinked polyethylene (UCAR TR-4202) and tree-retardant linear low-density polyethylene (UCAR TR-7521) introduced by Union Carbide Corp. Both are claimed to have higher dielectric breakdown strength and to resist or retard the rate of tree growth.

Many polymeric insulators are exposed to high levels of thermal stresses during their normal operations, since electrical power transmission generates heat. Thermal stresses not only change the properties of polymeric insulators, they also modify the structure of the materials. It is recognized that morphology of a polymeric insulator is one of the major material parameters that determine the final dielectric properties.[4-6] Therefore, it is extremely important to un-

Journal of Applied Polymer Science, Vol. 40, 263–283 (1990)
 CCC 0021-8995/90/1-20263-21$04.00

derstand the effects of thermal stresses on the morphology of polymeric insulators. Recently, a major study of the effect of annealing on crosslinked low density polyethylene (UCAR HFDE-4201) was reported.[7] In this paper the thermal aging behavior and the concurrent morphological developments of these recently introduced polyethylenes will be reported along with their general characteristics obtained mainly from infrared spectroscopy.

Studies of the morphological changes produced by annealing were carried out mainly by two techniques, small-angle X-ray scattering (SAXS) and differential scanning calorimetry (DSC). Small-angle X-ray scattering stems from the difference in electron density between the different entities inside materials. The regular stacking of entities of reasonably uniform thickness can cause the appearance of a discrete maximum in the SAXS pattern. The position of the peak then indicates the average repeat distance in the stacks of entities. A major feature of the long period spacing of polymeric materials is the dependence on the annealing or crystallization condition. Numerous studies of this phenomenon have been made, mostly for linear polyethylene.[8-11] The results of our studies will be compared with conventional polyethylene insulation materials.

EXPERIMENTAL

Materials

The materials used in this research are three different grades of crosslinked polyethylene and one grade of linear low-density polyethylene. Two of the three grades of XLPE are claimed to have superior dielectric properties and high resistance to the formation of water trees. All three grades are manufactured by Union Carbide Corp. especially for application as electrical insulation. The three XLPEs studied are (a) conventional HFDE 4201, (b) superclean HFDE 4201-EC, and (c) tree-retardant UCAR TR-4202. The linear low-density polyethylene also contains tree-retardant additives and is of special importance, since production of conventional LDPE for XLPE is more expensive than LLDPE and LLDPE may ultimately become a replacement material. There is a possibility that LLDPE, having a melting point 10°C higher than XLPE, will be able to function well enough without the necessity for crosslinking.

The specimens were prepared by compression molding; commercial pellets of XLPE obtained from the manufacturer being placed between two preheated platens at 135°C for about 10 minutes and pressed for a few minutes with an applied force of 20 tons to form initial molded sheets. The sheets were quenched to room temperature by plunging into water. The LLDPE samples were also prepared by compression molding using the above conditions, however, a molding temperature of 145°C was used.

Curing of XLPE was performed by holding the sample in a compression mold under the same force used for molding, but at 200°C for 5 minutes. The sheets were then quenched to room temperature by circulating cold water inside the platens. During curing, two sheets of polyimide film were placed at the upper and lower boundaries of the molten polymer and the preheated platen to reduce sticking. Small strips of sample were held at different aging temperatures for a prescribed period of time in an oil bath controlled to $\pm$ 0.5°C.

Characterization

Infrared spectroscopy was used to obtain information on chemical structure. All the infrared spectra were recorded on either a Digilab FTS-40 Fourier transform infrared spectrometer or a Perkin-Elmer 1330 infrared spectrophotometer.

All thermal experiments were carried out using a Perkin-Elmer differential scanning calorimeter model 7. The instrument was calibrated using the melting transition of pure indium at 156.6°C. DSC was used to measure heats of fusion, onset and peak temperatures of melting, and crystallinities. The DSC-7 was attached to a PE 7500 Professional Computer, all DSC data being collected and analyzed automatically. The DSC-7 operated with a temperature rate accuracy of $\pm$ 0.1°C/min.

The oxidative stability was measured by monitoring copper-induced oxidative induction times using the Perkin Elmer DSC-7 (ASTM D3895-80). The specimens were caged in preoxidized copper sample pans and covers, the specimen and reference being heated to 200°C at a constant rate of 10°C/min in a nitrogen environment. When the equilibrium of 200°C was reached, the atmosphere was switched to oxygen at the same flow rate of 40 cc/min. The sample was then held at a constant temperature until the oxidative exotherm was present in the DSC curve.

Small-angle x-ray scattering (SAXS) experiments were carried out on the 10-meter small-angle x-ray scattering camera at the National Center for Small-Angle Scattering Research at the Oak Ridge National Laboratory in Oak Ridge, Tennessee. The 10-meter camera utilizes a rotating anode x-ray source, crystal monochromatization of the incident beam, pin-hole collimation, and a two-dimensional position-sensitive counter, as described by Hendricks.[12]

Data for SAXS curves were collected from the 64 $\times$ 64 element detector and processed in the attached minicomputer. These data were plotted as contour maps as a function of scattering vector **K**. Figure 1 is a typical SAXS contour map from a specimen used in this work. Since there is no pronounced orientation in the samples, all data were radially averaged to obtain one-dimensional scattering data of intensity versus scattering angle. The specimen-to-detector distance used was 5.126 m. The angular resolution in this case is about 0.5 mrad corresponding to the scattering vector of 0.004 $Å^{-1}$. The scattering intensity has been corrected for cosmic radiation, unnecessary scattering from collimation slits, and possible nonuniform efficiency of the detector.

A comparison of dielectric strength of the series of XLPEs and TR LLDPE was performed using an ac breakdown strength test at a uniform rate of 1 kV/s until failure. The failure was evident by actual rupture of the specimen. Breakdown tests were carried out only with unaged samples. For TR LLDPE biaxially stretched samples were also prepared using a T. M. Long biaxial stretcher to investigate the influence of biaxial orientation on breakdown strength.

RESULTS

IR Spectra

Figure 2 illustrates infrared spectra obtained for the four materials in the 1800–600 cm^{-1} region. The relatively low intensity of the 1378 cm^{-1} band,

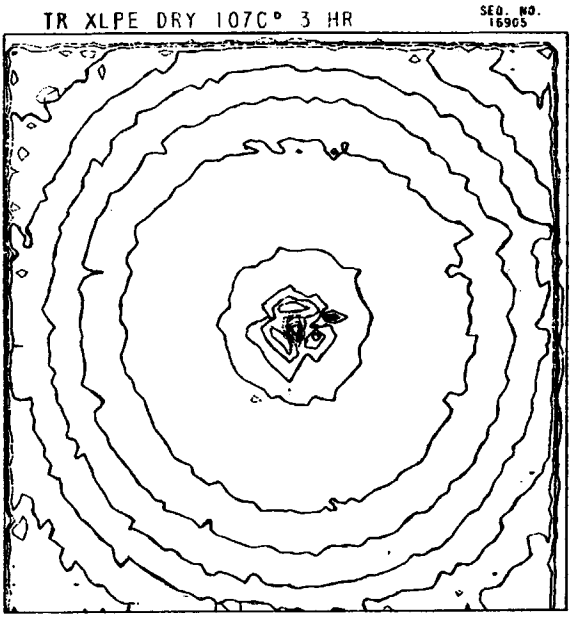

Fig. 1. Typical SAXS contour pattern of unoriented TR XLPE.

which is known to be directly proportional to the methyl group concentration, was observed for the tree-retardant (TR) LLDPE (TR-7501). This result indicates a lower level of short-chain branching for this material consistent with

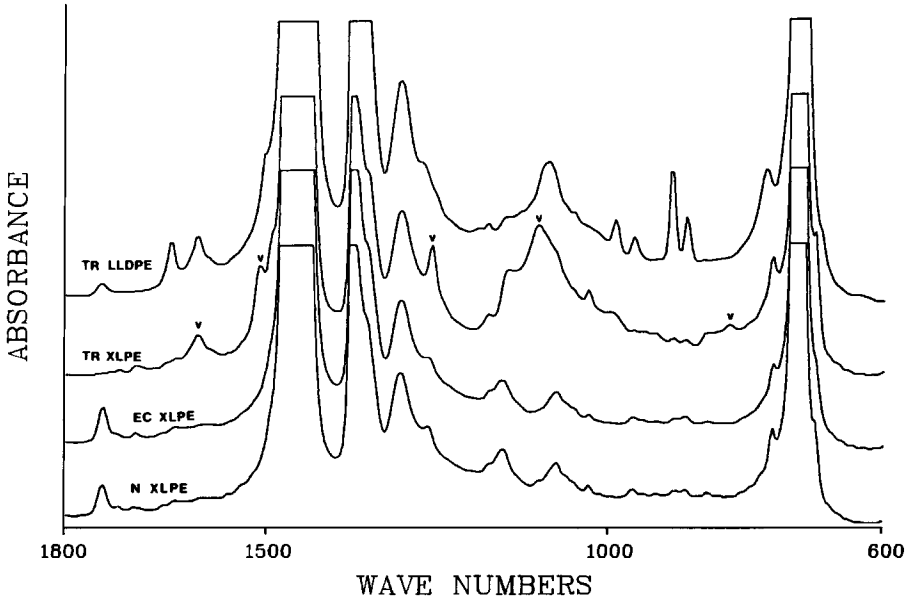

Fig. 2. Infrared absorption spectra of TR LLDPE, TR XLPE, extra-clean XLPE, and normal XLPE.

its copolymer structure. The amount of short branching is known to affect the melting point substantially,[13] a more randomly branched polymer having a lower final melting point and a sharper melting range. TR LLDPE also exhibits a higher degree of vinyl unsaturation (at 908 cm^{-1}) than vinylidene (880 cm^{-1}) or *t*-vinylene (963 cm^{-1}) unsaturation.

Extra-clean (EC) XLPE (HFDE-4201 EC) exhibits a pattern similar to that of normal (N) XLPE (HFDE-4201). Both show a typical band at ca. 1740 cm^{-1}, which arises from the acetophenone produced from the dicumyl peroxide during the crosslinking process. On the other hand, TR XLPE (TR-4202) exhibited several additional bands at ca. 1604, 1512, 1257, 1103, 1030, and 825 cm^{-1}. These bands are more pronounced in the difference spectra shown in Figure 3. Since such bands are usually associated with 1,4-substituted aromatic compounds, they are thought to arise from the tree retardant. Figure 4 illustrates a comparison of spectra of extractables, gel fraction, crosslinked, and uncured TR XLPE. The extractable fraction of TR XLPE exhibits a higher level of *t*-vinylene unsaturation and a relatively lower level of methyl and ethyl end groups; whereas the uncured material shows a higher level of vinyl unsaturation. The extractable fraction also shows a highly intense band at ca. 1720 cm^{-1}.

Differential Scanning Calorimetry

Even though differences in chemical additives are indicated in the infrared (IR) study, all three grades of XLPE show similar melting and annealing behavior. Figure 5 shows the changes in the DSC curve with increasing annealing temperature. As annealing temperature increases, the generation of multiple melting peaks occurs. To understand the phenomenon better, the melting curves of uncured, crosslinked, gel, and extractable fractions of TR XLPE have been studied and are presented in Figure 6. Uncured material as well as the extractable

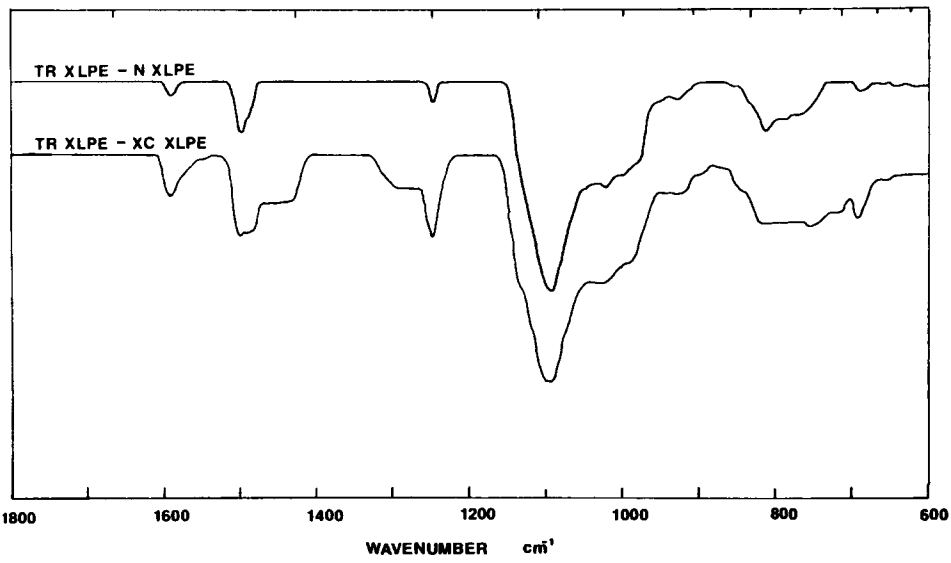

Fig. 3. Difference infrared spectra of extra-clean and normal XLPE subtracted from TR XLPE.

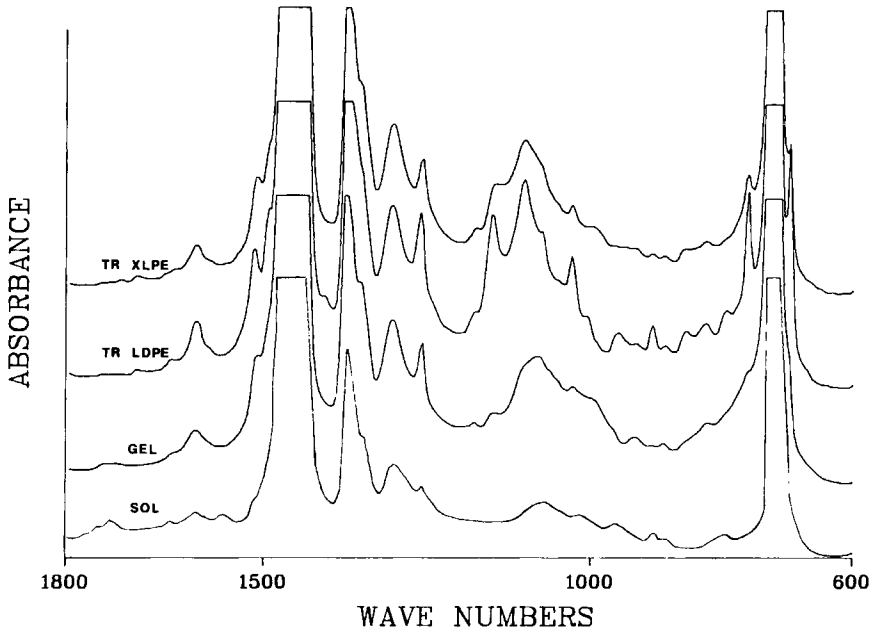

Fig. 4. Infrared absorption spectra of network, extractable, cured, and uncured TR-4202 PE.

or sol fraction of TR XLPE show a higher melting peak ($\sim$ 110°C), whereas the cured sample and the gel fraction show peaks around 103°C. This result is consistent with previous results obtained for normal XLPE.[14] It indicates a lowering of the melting point by crosslinking, but also that small fractions with high melting point are present even after curing. Although supercooling does

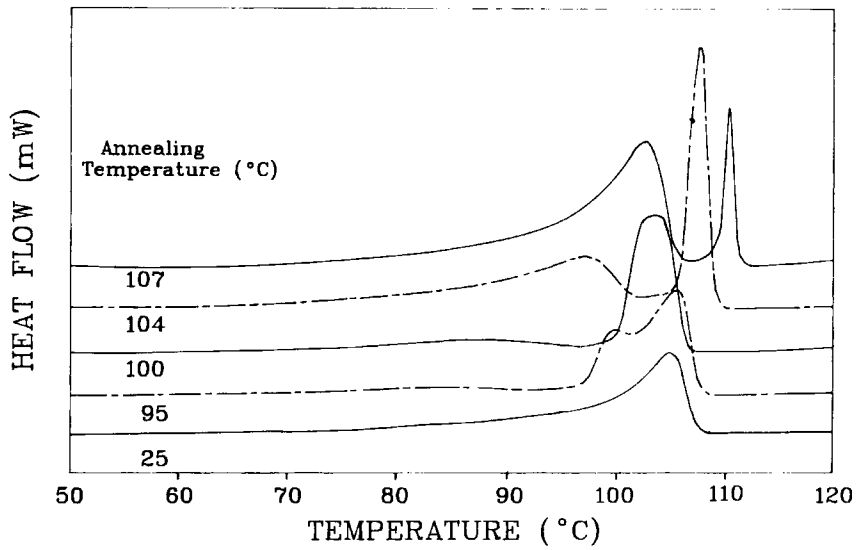

Fig. 5. DSC curves of TR XLPE annealed for 3 h at various temperatures.

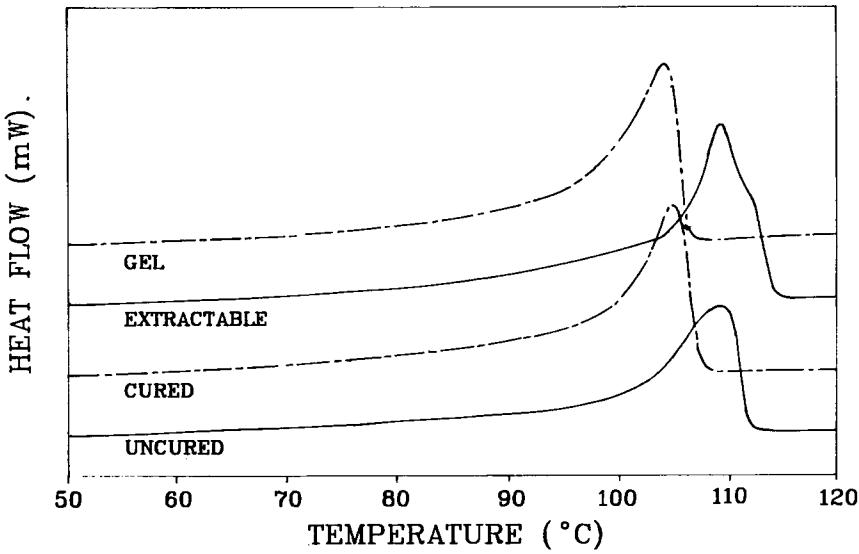

Fig. 6. DSC curves of network, extractable, cured, and uncured TR-4202 PE.

not allow this fraction to separate from the gel network, annealing gives sufficient time for separation to occur.

The effect of annealing time is illustrated in Figures 7, 8, and 9. At an annealing temperature where separation occurs, the gap between the two melting peaks increases with annealing time. The increase of the second peak temperature is illustrated in a semilog plot at annealing temperatures of 100 and 107°C (Figs. 7 and 8). Another important feature of the change in the DSC

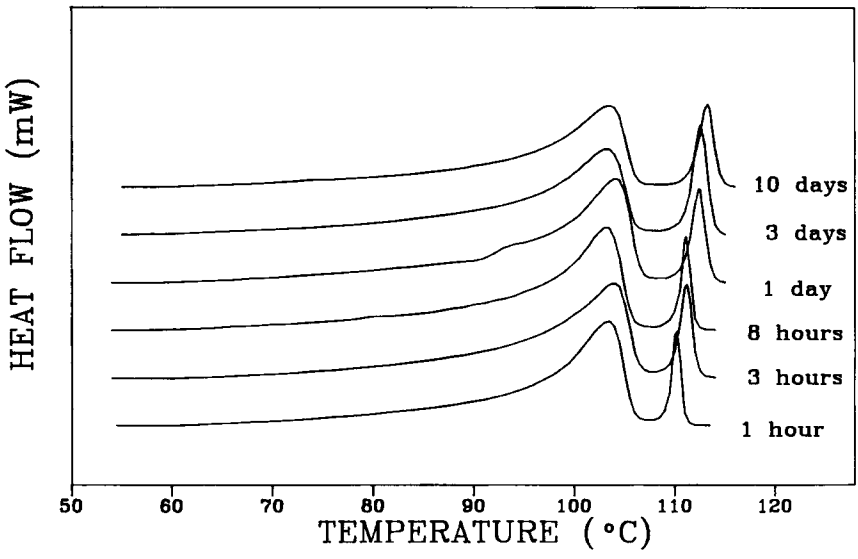

Fig. 7. Change in DSC curves of TR XLPE with annealing time at an annealing temperature of 107°C.

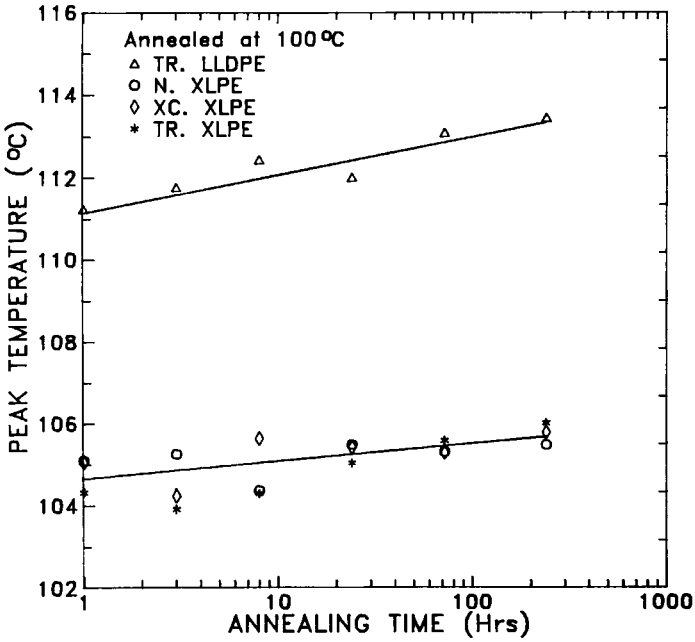

Fig. 8. Plots of second melting peak temperature as a function of annealing time at 100°C.

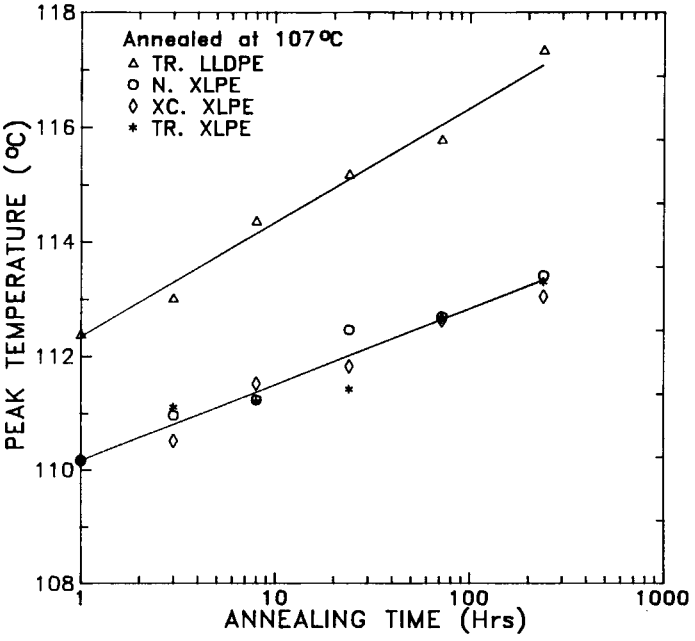

Fig. 9. Plots of second melting peak temperature as a function of annealing time at 107°C.

curve with annealing time is the variation of heats of fusion of each peak. The heat of fusion (ΔH_f) is an indication of the fraction of crystals present. As annealing time increases, the total ΔH_f and the ΔH_f of the peak located at a higher temperature show a steady increase, but that of the lower temperature peak shows some decrease. However, it is of interest that the incremental values of ΔH_f of the second peak are larger than the decrements of ΔH_f of the first peak. This finding suggests that the perfection of crystals associated with the second peak occurs at the expense of crystals melting in the first peak as well as at the expense of the amorphous content. The results are presented in Table I.

The melting behavior of TR LLDPE is quite different from that of the XLPEs. As indicated in Figure 10, the room temperature-quenched sample shows shoulders at temperatures above and below that of the major peak. Quenching in an ice bath or a dry ice-ethanol bath did produce a single broad peak. The slowly cooled TR LLDPE, interestingly, shows two completely separated peaks, one being sharper and at a higher temperature than the other. These results are at least as complex as those for XLPE but of different origin. They may be caused by crystals having different levels of branching in their molecules. With increasing annealing temperature, a complicated melting peak pattern developed. At relatively high annealing temperatures ($\sim$ 112–120°C), TR LLDPE exhibits major separation of melting peaks, the lower broad peak being produced by material unable to crystallize at the annealing temperature

TABLE I
Variation of Heat of Fusion of Each Peak with Annealing Time

	Annealing condition	Total ΔH (J/g)	First ΔH (J/g)	Second ΔH (J/g)
TR XLPE	Uncured	116	0	116
	Cured but fresh	117	117	0
	107C/1 h	103	91	11
	107C/3 h	108	91	17
	107C/8 h	108	87	21
	107C/3 days	110	87	23
XC XLPE	Uncured	118	0	118
	Cured but fresh	118	118	0
	107C/1 h	104	89	14
	107C/3 h	105	99	7
	107C/8 h	110	86	24
	107C/3 days	115	90	24
N XLPE	Uncured	124	0	124
	Cured but fresh	114	114	0
	107C/1 h	102	96	6
	107C/3 h	101	96	5
	107C/8 h	110	70	41
	107C/3 days	111	67	44
TR LLDPE	Unaged	119	0	119
	107C/1 h	115	52	63
	107C/3 h	116	49	67
	107C/8 h	115	45	70
	107C/3 days	122	49	74

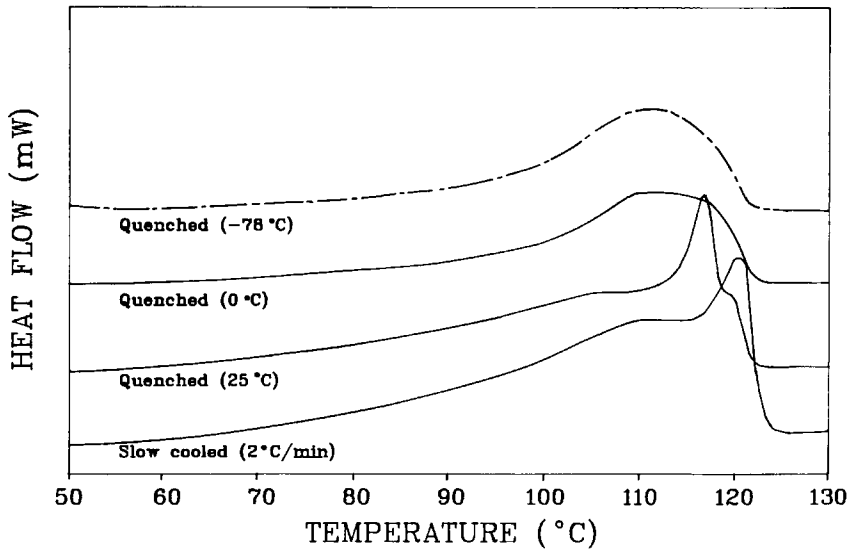

Fig. 10. DSC curves of TR LLDPE solidified under conditions indicated.

(Fig. 11). The time dependence observed at the annealing temperature of 117°C is, however, similar to those observed for XLPEs annealed at 107°C (Fig. 12).

Small-Angle X-Ray Scattering

SAXS data were collected for the three grades of XLPE and the LLDPE, all annealed at 107°C for prescribed periods of time. Figures 13, 14, 15, and 16 are radially averaged intensity plots obtained from SAXS intensity contour

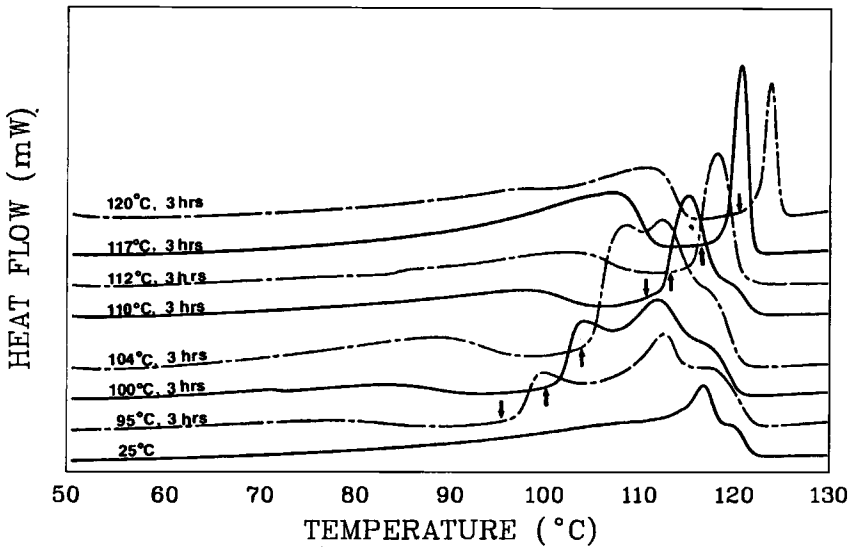

Fig. 11. Variation of DSC curves of TR LLDPE annealed for 3 h at the indicated temperatures.

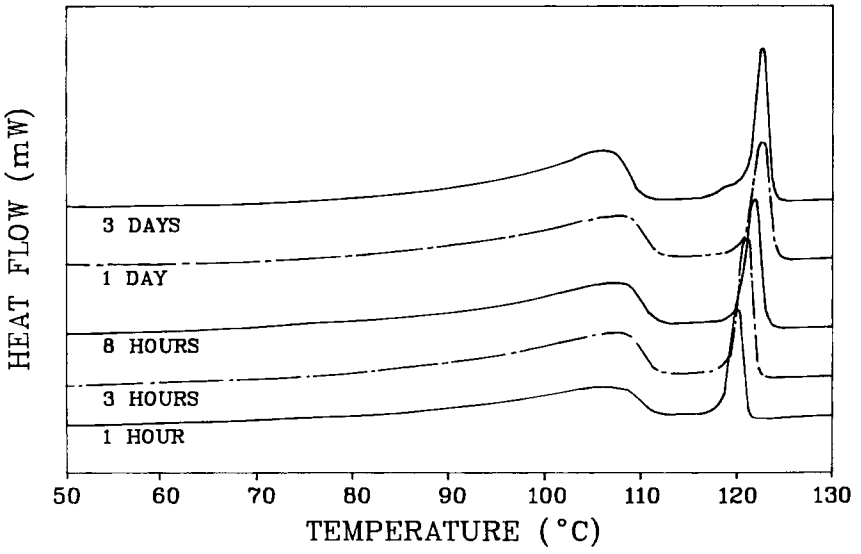

Fig. 12. Change in DSC curves of TR LLDPE with annealing time at annealing temperature of 117°C.

plots. The general shapes of SAXS curves of XLPE are quite different from that of TR LLDPE. The SAXS plots of XLPE show well defined Bragg maxima, indicating the presence of stackings of two entities of differing electron density,

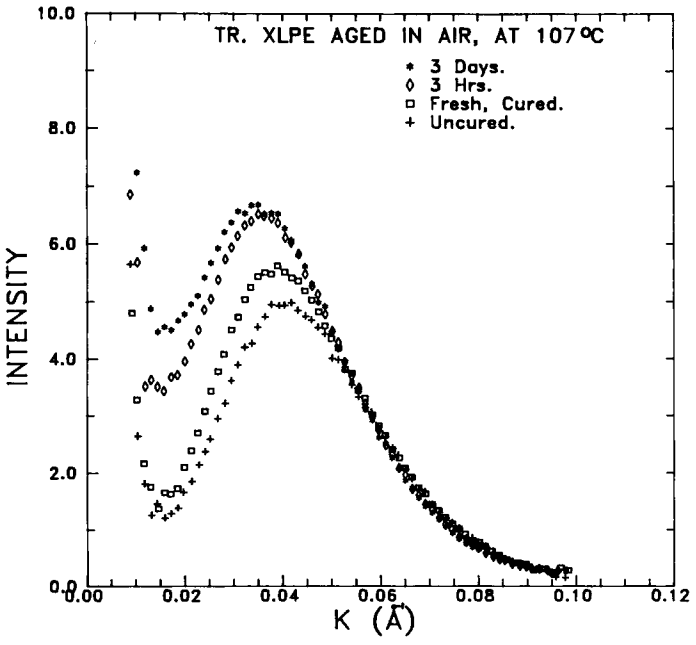

Fig. 13. Variation of radially averaged SAXS intensity curves of TR XLPE with annealing time at 107°C.

presumably amorphous and crystalline layers (Figs. 13, 14, and 15). On the other hand, the intensity curves of TR LLDPE show less well-defined maxima. Such intensity curves may indicate the presence of a poorly defined stacking structure with a wide distribution of size (Fig. 16).

Even though the shapes of the intensity curves of the XLPEs differ from that of TR LLDPE, the effects of annealing time on these two polyethylenes are similar. One sees three principal effects. First, with increasing annealing time the Bragg maxima move toward lower angles, indicating an increase in long period spacing. Such an effect is known to be common in annealed linear polymers.[15]

A second effect is a general increase of intensity as the annealing time increases. This effect is more clearly shown in the subtracted plots where the intensity values of the unannealed sample were subtracted from those of the annealed samples (Figs. 17 and 18). One can see clearly that the major enhancement of intensity with annealing occurs at lower angles near the beam stop, with the maximum of subtracted intensity being at the angle just below the Bragg maximum. It has been proposed that the intensity near the beam stop, referred to as zero-angle intensity, is associated with amorphous gaps in the lamellar stacking.[16] It also can be speculated that the scattering intensity up to 0.015 $Å^{-1}$ of scattering vector arises from entities larger than 400 Å, such as microvoids, impurities or super thick lamellae embedded inside the material.

The third effect is that the breadths of the peaks narrow with annealing. The narrowness of a peak arises from an increase in the regularity of lamellar stacking and can be attributed to the distribution of stack size. Not surprisingly, this effect has been reported in the crystallization of high-density polyethylene.[6,8]

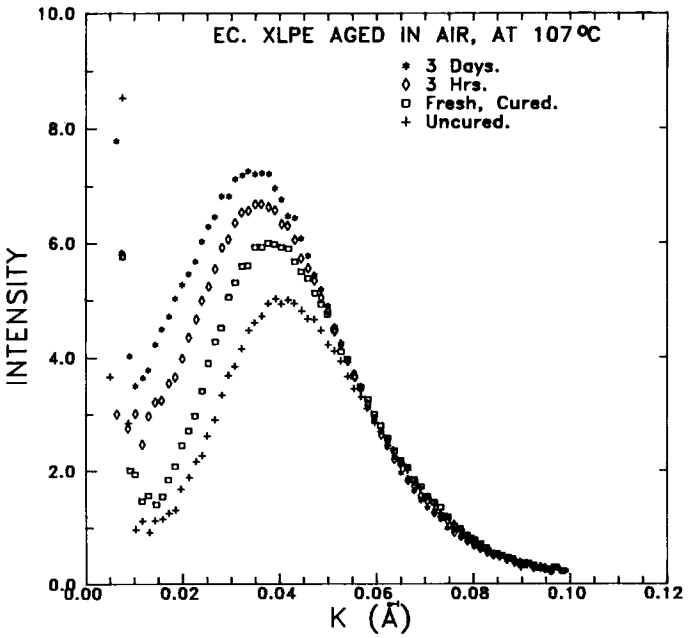

Fig. 14. Variation of radially averaged SAXS intensity curves of extra-clean XLPE with annealing time at 107°C.

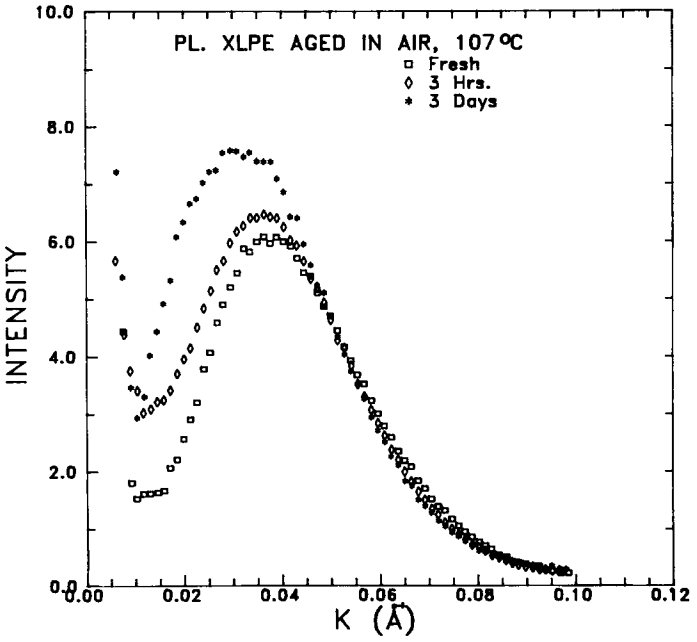

Fig. 15. Variation of radially averaged SAXS intensity curves of normal XLPE with annealing time at 107°C.

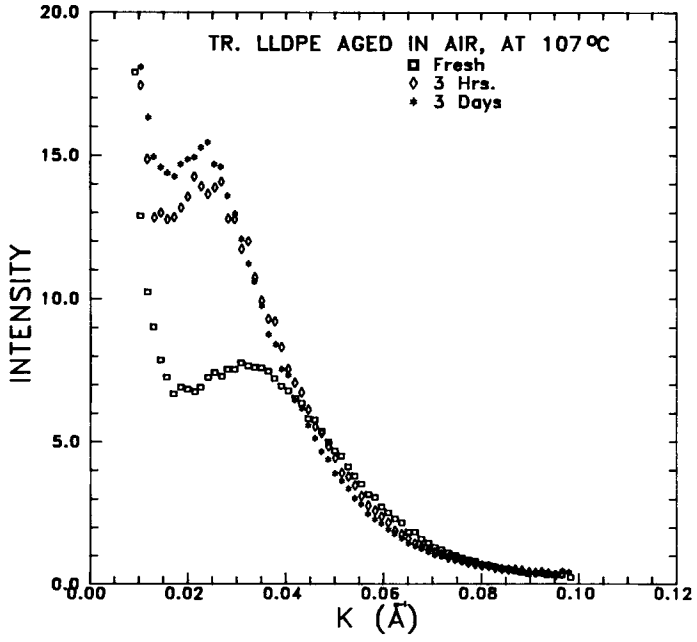

Fig. 16. Variation of radially averaged SAXS intensity curves of TR LLDPE with annealing time at 107°C.

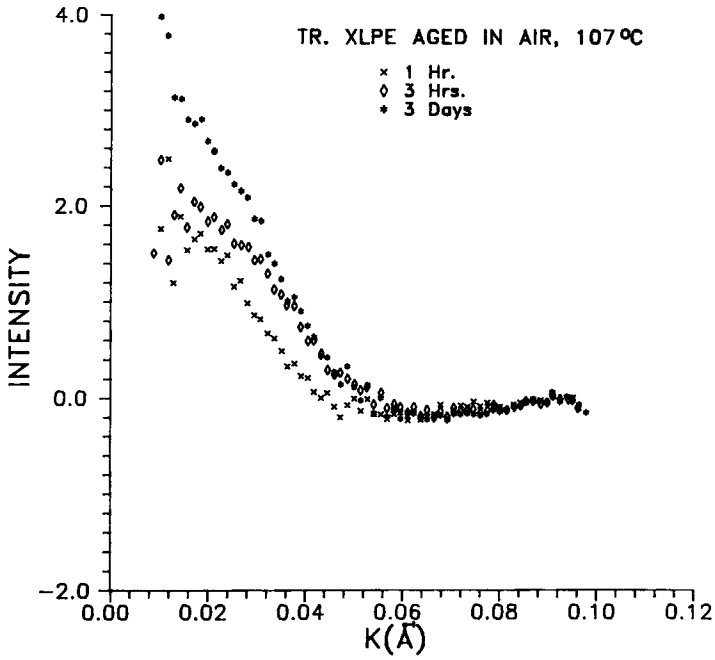

Fig. 17. SAXS intensity difference curves between TR XLPE annealed at 107°C and untreated TR XLPE, as a function of annealing time.

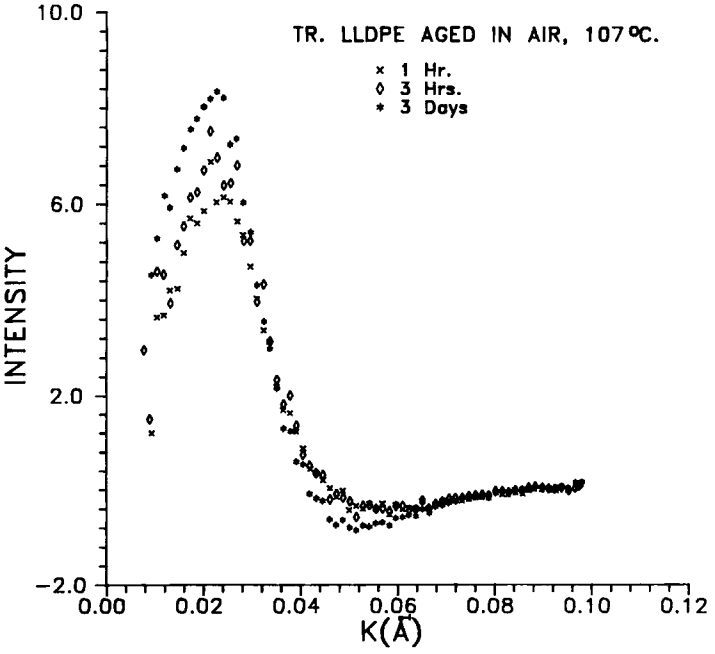

Fig. 18. SAXS intensity difference curves between TR LLDPE annealed at 107°C and untreated TR LLDPE, as a function of annealing time.

It is also of interest to note that curing results in effects similar to those of annealing. Once cured, the sample shows an increase in the Bragg maximum and overall intensity and sharpening of the Bragg peak.

The long period spacing is known to be an average value of total thickness of crystallites and amorphous portions, provided that a model consisting of alternating crystalline and amorphous regions in the direction of the lamellar axis is appropriate. The crystallinity can be calculated from the DSC results as the ratio of a heat of fusion of a specific sample to that of a theoretically 100% crystalline polyethylene (Table II). Interestingly, curing results in an increase in thickness of the crystalline layer with a relatively smaller increase in the amorphous layer. However, all annealed XLPEs show a thicker amorphous layer (ca. 85 Å) than the unannealed specimens (ca. 65 Å). An additional feature of LLDPE is that with annealing time major thickening occurs in the crystalline layer with a relatively constant value of the thickness of the amorphous layer.

Electric Breakdown Strength

Specimens with thicknesses of 1 to 4 mil (25–100 μm) were prepared by compression molding for electric breakdown testing. All specimens were unaged in order to investigate differences in as-molded breakdown strength. For TR LLDPE, biaxially stretched specimens were also prepared using a T. M. Long

TABLE II
Variation of Thickness of Crystalline and Amorphous Layers with Annealing Time at 107°C

	Sample condition	SAXS long period (Å)	Crystallinity (%)	Crystal thickness (Å)	Amorphous thickness (Å)
TR XLPE	Uncured	153	57.0%	87	66
	Cured	161	57.8%	93	68
	107C/1 h	173	50.5%	88	86
	107C/3 h	177	53.0%	94	83
	107C/8 h	177	53.1%	94	83
	107C/3 days	180	54.0%	97	83
XC XLPE	Uncured	156	57.9%	90	66
	Cured	164	58.2%	95	69
	107C/1 h	166	51.1%	85	81
	107C/3 h	177	51.9%	92	85
	107C/8 h	180	54.2%	98	83
	107C/3 days	180	56.5%	102	78
N XLPE	Uncured	167	61.2%	102	65
	107C/1 h	173	50.1%	87	87
	107C/3 h	173	49.9%	86	87
	107C/8 h	184	54.5%	100	84
	107C/3 days	191	54.8%	105	86
TR LLDPE	Unaged	204	58.7%	120	84
	107C/1 h	255	56.5%	144	111
	107C/3 h	262	57.3%	150	112
	107C/8 h	261	56.9%	149	113
	107C/3 days	271	60.2%	163	108

stretch machine following compression molding. The Weibull distribution plots of ac breakdown strength of TR and EC XLPEs and TR LLDPE are compared in Figure 19. All XLPEs and unstretched TR LLDPE show a more or less similar distribution. TR XLPE shows a higher value of the scale parameter ($\sim$ 3.6 kV/mil), which corresponds to the average value of the standard distribution, than EC XLPE (3.0 kV/mil). TR XLPE also shows a significant curvature to the Weibull plot, such as has been seen in studies of XLPE annealed at high temperatures.[17,18] TR LLDPE also shows a relatively higher value of scale parameter ($\sim$ 3.3 kV/mil). This finding is matched, to some degree, with the claim of the manufacturer that TR grade shows higher breakdown strengths. It is noteworthy that the biaxially stretched TR LLDPE has the highest BD strength with a scale parameter of 5.3 kV/mil. This may be due to a thickness effect as well as an orientation effect since the biaxially oriented specimen was half as thick as the other specimens.

Oxidative Induction Time

Oxidative induction time (OIT) is a relative measure of the level of oxidative stabilization of the material tested. OIT was determined for all freshly prepared samples in the presence of oxygen at 200°C. DSC curves were recorded in a plot with the time on the x axis. The results are presented in Figure 20. The striking feature is that EC-4201 or normal HFDE-4201 show instantaneous oxidative exotherms. On the other hand, TR-grade polyethylenes such as TR-4202 and TR-7512 show oxidative induction times of 4.7 and 7.5 minutes, respectively.

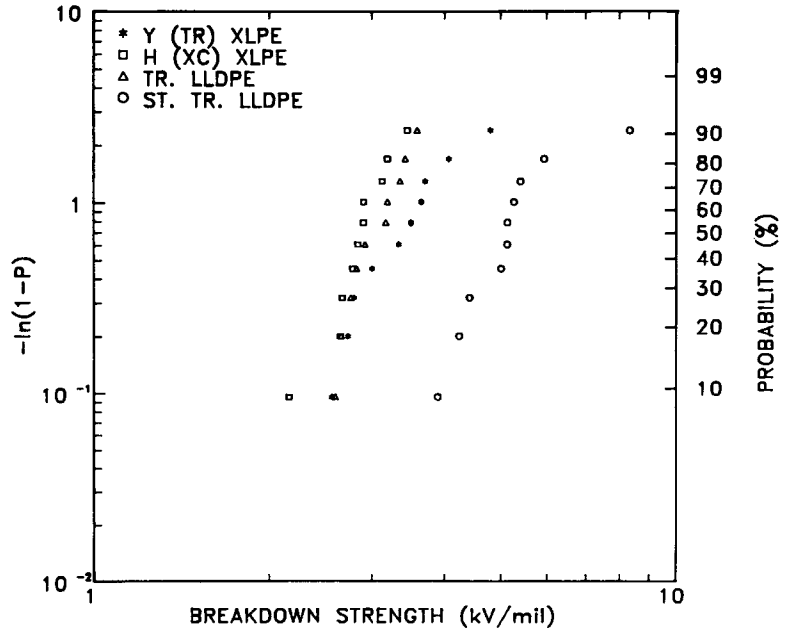

Fig. 19. Weibull distribution plots of breakdown strength of TR XLPE, EC XLPE, TR LLDPE, and biaxially stretched TR LLDPE.

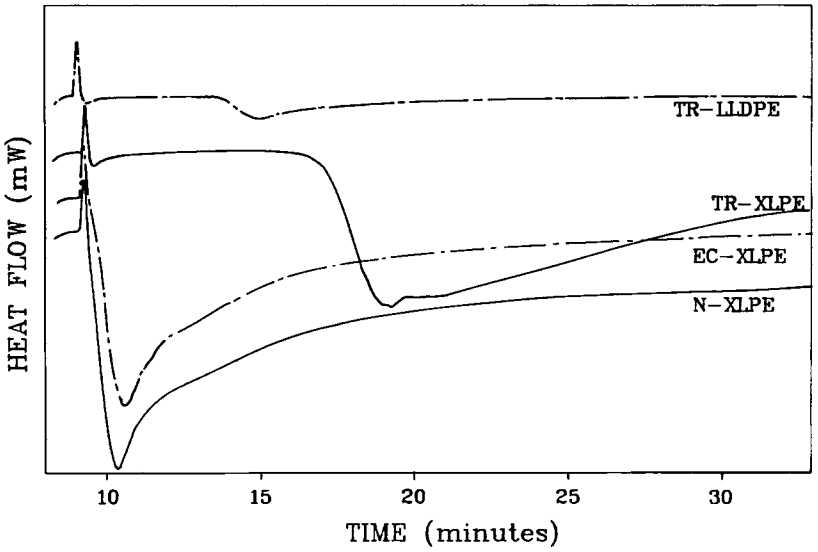

Fig. 20. Isothermal oxidative thermograms for TR LLDPE, TR XLPE, EC XLPE, and N. XLPE at 200°C in an oxygen environment.

The other finding to note is that the oxidation reactive exotherm of XLPE is much larger than that of LLDPE. This may indicate that XLPE will be damaged more by oxidation than LLDPE for equivalent exposure.

DISCUSSION

It has been claimed that TR-4202 is more resistant to electrical aging than the HFDE-4201 by Turbitt[19] and Chan.[20] They also reported that TR-4202 has a higher breakdown strength in its original state. As shown in the preceding section, results of electrical breakdown strength testing agree with their results. Since the major difference between TR XLPE and normal XLPE is the presence of the chemical additive, the enhancement of the electrical properties appeared to be due to the additive. Moreover, the OIT analysis shows that TR grade polymer exhibits a longer oxidative induction time. Therefore, it can be inferred that the chemical additive has dual functions—antioxidant and tree retardant. It is also known that electrical rupture and consequent damage can be characterized as a thermo-oxidative degradation process.[21–23] Since antioxidant normally works as an electron acceptor, it provides some voltage stabilizer activity in addition to its normal role of retarding polymer oxidative degradation.

First, the series of XLPEs will be considered. It is known that the only difference in production of HFDE 4201-EC compared to HFDE 4201 is that great care is taken in the prevention of solid particle contamination. There are no special chemical additives present. The situation is quite different for TR 4202 where a liquid antioxidant has been used together with an additional chemical bonded to the polymer chain. This latter adaptation is designed to function in the same way as acetophenone is believed, by some, to function in XLPE. It is known that XLPE, once having lost its acetophenone byproduct,

is much more susceptible to tree initiation than when freshly made. This resistance may be caused by the acetophenone reacting chemically, partially filling voids or acting as a surfactant in trees, incipient or otherwise. The additive, which has a similar chemical function to acetophenone, is bonded to the chain so that it cannot be lost by diffusion to the environment. It is believed to be added as a comonomer during synthesis. As such it might influence the level of chain branching in the polymer as well as the crystallization and annealing behavior. There is only a small level of difference, if any within the limit of experimental error, in heats of fusion of TR XLPE from the other groups of XLPEs. The lower value of heat of fusion of TR XLPE may represent a slightly lower crystallinity. The general lower SAXS intensity of this material also supports the above speculation.

It will be recalled that the infrared spectra showed that the extractable fraction had higher levels of *t*-vinylene unsaturation and lower levels of branching than the gel fraction. The uncured material showed a high vinyl content. It is possible that the vinyl group of a major additive reacts and is bonded into the gel network. The major differences in IR spectra between 4201 and TR 4202 lie in the peaks present at 1103, 1257, and 1604 cm^{-1}. Also notable is the low magnitude small peak at 1740 cm^{-1}. The magnitudes of these peaks vary from extractable to gel fraction (Fig. 4). The extractables alone show the 800 and 1740 cm^{-1} absorptions, the peaks at 1000, 1103, 1257, and 1570 cm^{-1} are enhanced over the gel. Clearly one segment of additive is extractable and a second has been attached to the network. The peaks at 1103, 1257, and 1604 cm^{-1} do, however, appear for both extractable and gel fractions and so some chemical groups, if not entire additives, are present in both components of the final product.

The major response to thermal aging treatments of all XLPEs is thickening of crystals as well as amorphous layers (Table II). Once cured at a temperature near the melting point, all grades of XLPE show a sudden increase of the amorphous layer of about 20 Å. However, as annealing time at 107°C increases from 1 h to 3 days, the amorphous layer shows little or no change in thickness. Some samples show a slight decrease in amorphous thickness. On the other hand, the thickness of the crystal layer increases steadily with annealing time from ca. 90 to ca. 100 Å. This thickening was accompanied with a refinement of the crystal layers.

Another striking structural feature of thermal aging of XLPE is the change in zero-angle intensity. The intensity near the beam-stop (up to scattering vector 0.0125 $Å^{-1}$) shows a steady increase with curing as well as annealing. For linear polyethylene, however, it was reported that the zero-angle intensity showed a slight decrease with increasing crystallization time.[6,8] The diminishing of zero-angle intensity with crystallization time was asserted to be due to the growth of new crystallites within the amorphous gap.[8] If this assertion is true for crystallization of polyethylene, then the slight increase of near zero-angle intensity observed in annealing in XLPE suggests that the growth mechanism of crystallites during annealing of XLPE is different from that of linear polyethylene.

Another minor difference among the crosslinked polyethylenes lies in the magnitude of the high temperature peak produced by high temperature annealings (e.g., 107°C) of the tree-retardant material compared with normal

XLPE. It is reproducibly of slightly higher magnitude, suggesting that it is slightly easier for sol-gel separation to take place in the melt in TR-4202 than in 4201. The chemical differences between the sol and gel phases might provide the extra driving force in free energy difference needed.[24]

Secondly, the tree-retardant LLDPE will now be considered. The IR spectra show that the chemical additives present in the LLDPE are very similar to those used in the 4202-TR XLPE. Notable, however, is the presence of an enhanced vinyl content at 908 cm^{-1} which is considerably larger than in the uncrosslinked 4202-TR, indicating either a different formulation or an abnormally high vinyl content in the polymer molecules of the LLDPE.

LLDPEs are copolymers of ethylene with unsaturated hydrocarbons longer than ethylene. Commonly butene is used along with octene or hexene, etc. It is known that a distribution of copolymer content exists among the molecules, some being essentially linear polyethylene while others have a high comonomer content. Such structural variations can be expected to have a major influence on the crystallization process since fractionation, according to comonomer content, is predicted. The difficulty in producing a single broad melting peak on quenching is a symptom of this phenomenon. Only a drastic method such as ethanol-dry ice bath quenching produced a relatively conventional melting peak, however, it was also much broader than is usually observed for LDPE's. Fractionation on crystallization is much more clearly shown in the DSC curve of slow cooled (cooling rate 2°C/min) TR LLDPE (see Fig. 10) where one broad peak is located at 109°C along with a major sharp peak at 125°C. This type of behavior is not uncommon, since there is enough time for fractionation during slow cooling. The melting curve of insulation produced from this material is likely to be similar to that produced by a room temperature quench (i.e., complex). It should therefore show a long tail beginning at ca. 60°C leading to an important shoulder at ca. 105°C, a peak at 115°C, and a final end of melting at about 122°C.

The consequences of this melting curve are major for thermal aging and perhaps also for useful operating temperature ranges since the insulation is likely to retain its structural integrity up to at least 115°C.

Annealing causes major changes in the DSC curves (see Fig. 11). Although a low temperature hump appears, symptomatic of material that cannot crystallize at the annealing temperature, it is not of major significance unless the temperature is greater than ca. 115°C. Hence most of the material recrystallizes during annealing, in contrast to XLPE. The production of the hump coincides with the emergence of a sharp high melting peak. The temperature of this peak is very sensitive to the annealing temperature, generally being located ca. 3°C above the annealing temperature. It is similar in appearance to the peak observed at ca. 107°C in XLPE. In all likelihood it is produced by the most linear molecules present and indicative of fractionation according to branching. Since the temperature of the peak is sensitive to annealing time (Fig. 12), it is likely that the crystals are able to thicken appreciably. The SAXS data show this symptom very clearly. Even one hour of annealing results in thickening of up to 20 Å (see Table II). The melting point of linear polyethylene is usually in the range 130–135°C, whereas that of branched polyethylene is ca. 105°C.

It is not known how this behavior will influence dielectric breakdown and tree resistance. Studies on XLPE showed that annealing below the melting

peak resulted in considerably reduced tree resistance and dielectric breakdown strength.[18,24] Annealing above the melting peak produced an enhanced breakdown strength. If such a situation recurs here, the breakdown strength might be reduced for annealing temperatures up to 115°C, whereas for XLPE improved properties resulted for annealing at 100°C and above. Conversely, annealing at 90°C and below may have little effect on LLDPE. Only additional experimentation can resolve the issue.

Finally, a few comments will be made regarding the electrical and OIT testing. Clearly, there is a strong inverse correlation between the slopes of the Weibull plots of breakdown strength and the oxidation induction times. The tree-retardant XLPE shows the lowest slope in the Weibull plot and the longest OIT, whereas the extra-clean XLPE shows the highest slope and the shortest OIT. Tree-retardant LLDPE falls between the two. Since the Weibull plot is a probability of failure plot, it can be stated that although all three materials show similar values of the lowest observed breakdown strength, they differ considerably in the value of breakdown strength characteristic of a high probability failure. From these studies, it would appear that oxidation is a major contributor to dielectric breakdown and that antioxidants have a major influence on breakdown strength. The biaxially oriented TR-LLDPE showed the highest breakdown strength. It differed from the unoriented material through the value of the inception voltage (i.e., the lowest voltage at which failure occurred) and not through the slope of the Weibull plot. A possible conclusion from this study might be that the slope of the Weibull plot is determined largely by oxidative stability, but that the inception voltage is most sensitive to morphological factors.

We are grateful for the use of the SAXS facility at Oak Ridge National Laboratory and for many useful discussions with Dr. J. S. Lin.

References

1. R. M. Eichhorn, Kabelitems, No. 157, Union Carbide Corp. (1981).
2. J. M. Braun, *IEEE EI-15,* 120–123 (1980).
3. R. M. Eichhorn, *Engineering Dielectrics,* Vol IIA, ASTM, STP 783, Philadelphia, PA, 1983, pp. 355–444.
4. T. Fukuda, S. Irie, Y. Asada, M. Maeda, H. Nakagawa, and N. Yamada, *IEEE 1980* Conf. Rec. of Electr. Ins., 1981, pp. 118–121.
5. S. V. Kolesov, *IEEE EI-15,* 382-388 (1980).
6. B. V. Ceres and J. M. Schultz, *J. Appl. Polym. Sci.,* **29,** 4183–4197 (1984).
7. P. J. Phillips and A. Vatansever, *Polymer,* **30,** 711–717 (1989).
8. R. G. Brown and R. K. Eby, *J. Appl. Phys.,* **35,** 1156–1161 (1964).
9. J. Dlugosz, G. V. Fraser, D. Grubb, A. Keller, J. A. Odell, and P. L. Goggin, *Polymer,* **17,** 471–480 (1976).
10. J. M. Schultz, J. S. Lin, and R. W. Hendricks, *J. Appl. Cryst.,* **11,** 551–557 (1978).
11. M. J. McCready, J. M. Schultz, J. S. Lin, and R. W. Hendricks, *J. Polym. Sci., Polym. Phys.,* **17,** 725–740 (1979).
12. R. W. Hendricks, *J. Appl. Cryst.,* **11,** 15 (1978).
13. F. P. Reding, *J. Polym. Sci.,* **32,** 487 (1958).
14. P. J. Phillips and A. Vatansever, *Polym., Comm.,* **25,** 204–206 (1984).
15. L. E. Alexander, *X-ray Diffraction Methods in Polymer Science,* Wiley Interscience, New York, 1969.
16. J. M. Schultz, *J. Polym. Sci. Polym. Phys. Ed.,* **14,** 2291–2311 (1976).

17. P. J. Phillips and A. Vatansever, submitted for publication.

18. Final Report (EL-5921) on EPRI Contract RP 7891, The Morphology of Crosslinked Polyethylene Cable Insulation and Its Influence on Breakdown Strength, EPRI, Palo Alto, CA, 1988.

19. R. J. Turbitt, New Long Life Insulation Compound for URD Cables, Kabelitems No. 158, Union Carbide, 1984.

20. J. C. Chan, Aging Performance of Miniature Cable Extruded with a Commercial Tree Retardant XLPE Insulation, CEIDP 1984, 296–301, 1984.

21. Y. D. Lee and P. J. Phillips, *IEEE EI,* submitted.

22. A. Gorton, S. S. Bamji, A. Bulinski, and J. Densley, Oxidation and Water Treeing in XLPE Cable Insulation, 1986 CEIDP 404–410, 1987.

23. N. Shimizu, K. Uchida, and K. Horii, Initiation Mechanism of Electrical Tree-Chain Scission by Injected Charge and Role of Oxygen, 1987 CEIDP, 419–424, 1988.

24. P. J. Phillips and A. Vatansever, Polym. Eng. Sci., to appear.

Received October 6, 1988
Accepted June 21, 1989